CHARGED-PARTICLE TRACKING IN HEAVY-ION COLLISIONS FOR ATLAS IN RUN 4*

Luthien Mlynarska

on behalf of the ATLAS Collaboration

AGH University of Krakow, al. Mickiewicza 30, 30-059 Kraków, Poland
mmlynar@protonmail.ch

Received 27 March 2025, accepted 2 April 2025, published online 26 June 2025

The High Luminosity Large Hadron Collider (HL-LHC) will provide additional challenges in the already demanding field of charged-particle-track reconstruction. The Inner Detector of the ATLAS experiment will be replaced by an all-silicon Inner Tracker (ITk) that will consist of pixel and strip subdetectors providing greater coverage in pseudorapidity spanning up to $|\eta| = 4$. The physics of heavy ions (HI) requires a different tracking setup as compared to *pp* collisions. This is dictated by the difference in experimental conditions, where instead of a huge number of simultaneous *pp* interactions per bunch crossing (up to $\langle\mu\rangle = 200$), the HI collision events expect only one collision per bunch crossing. Despite this, a central lead-ion collision produces a huge number of charged particles to reconstruct, comparable to *pp* collisions at $\langle\mu\rangle = 200$. The presence of a single collision vertex enables certain optimizations but also introduces unique challenges. The ATLAS experiment has chosen A Common Tracking Software (ACTS) for the HL-LHC to perform track reconstruction, as it is expected to meet the new challenges ahead. This document highlights the progress in setting up the ACTS-based track reconstruction for HI with the ITk, shows a comparison of expected tracking performance in *pp* and HI events, and presents the predicted performance of ACTS compared to the existing tracking algorithms used by ATLAS.

DOI:10.5506/APhysPolBSupp.18.5-A23

1. Introduction

In 2030, the HL-LHC Run 4 is planned to start [2]. It will feature much higher instantaneous luminosity and pileup[1] (up to $\langle\mu\rangle = 200$) during

* Presented at the 31st Cracow Epiphany Conference on the *Recent LHC Results*, Kraków, Poland, 13–17 January, 2025.

[1] Pileup in that context stands for the number of simultaneous elementary inelastic proton–proton interactions during one bunch crossing and is characterised by the Poisson distribution with mean denoted as $\langle\mu\rangle$.

proton–proton (pp) collisions compared to the current maximum pileup up to $\langle\mu\rangle = 75$. In order to fully benefit from the increased luminosity, ATLAS [3] will undergo several upgrades of its detector parts, software, and trigger. The current Inner Detector (ID) will be replaced by the Inner Tracker (ITk) [4]. The ITk will have a coverage of $|\eta| \leq 4.0$ in pseudorapidity and will consist of pixel and strip subdetectors immersed in a 2T solenoidal magnetic field.

During each LHC data-taking period, heavy-ion collisions are also conducted. The conditions during HI collisions are quite different compared to pp. Firstly, no pileup is expected during the bunch crossing. This means that all primary particles originate from a single vertex. Secondly, the number of created charged particles is highly sensitive to the stochastically varying collision centrality, spanning over several orders of magnitude, while for pp at $\langle\mu\rangle = 200$, it is distributed around ~ 2000 with a standard deviation of $\sigma \sim 300$.

From the software side, A Common Tracking Software (ACTS) [5] is presently being developed and implemented into the ATLAS Software package, Athena [6].

2. Simulation and reconstruction

The results shown in this document are obtained using two Monte Carlo samples. For pp collisions, $t\bar{t}$ events generated using Powheg Box v2 [7–10] and NNPDF3.0nlo [11] at $\sqrt{s} = 14$ TeV centre-of-mass energy were used. A HI sample was generated using the Hijing generator [12] at $\sqrt{s_{NN}} = 5.36$ TeV. This sample contains lead–lead (Pb–Pb) collisions with centralities following a minimum-bias distribution. The simulated events are processed through the full ATLAS detector simulation [13] based on the Geant4 toolkit [14]. It uses the 03–00–01 detector layout [15]. Track reconstruction begins with the clustering of raw detector signals [16]. This step is required in order to determine the point of particle intersecting with tracking detector sensors. The 2D cluster positions are then converted to 3D space points. After the space-point creation, they are grouped into seeds, each consisting of 3 space points. Those seeds indicate initial parameters for the Combinational Kalman Filter algorithm and are further propagated while constructing the complete track trajectory using measurements from all detector layers. Due to the large number of track candidates, the ambiguity resolution algorithm is applied before passing into the final precision fit. The final collection of reconstructed tracks has to fulfill a list of requirements, which are optimised for the event type and are shown in Table 1. The η-dependent requirements have been optimized for the pp reconstruction, while the same requirements are applied over the full η range in the case of HI collisions.

Table 1. Set of requirements applied during the track reconstruction in different pseudorapidity intervals for pp and Pb–Pb events. A hole is an intersection of the predicted particle's trajectory with an active sensor element from which no measurement is assigned to the track (inactive sensors are not taken into account). The hole counting does not consider layers before the first and after the last hit. z_0 and d_0 refer to the longitudinal and transverse impact parameters, respectively, and are defined with respect to the mean position of the beam spot.

Requirements	pp			Pb–Pb
	$\lvert\eta\rvert \leq 2.0$	$2.0 < \lvert\eta\rvert \leq 2.6$	$2.6 < \lvert\eta\rvert \leq 4.0$	$\lvert\eta\rvert \leq 4.0$
Pixel+strip hits	≥ 9	≥ 8	≥ 7	≥ 6
Pixel hits	≥ 1	≥ 1	≥ 1	≥ 1
Holes	≤ 2	≤ 2	≤ 2	≤ 2
p_{T} [MeV]	> 900	> 400	> 400	> 400
$\lvert d_0\rvert$ [mm]	< 2.0	< 2.0	< 10.0	< 2.0
$\lvert z_0\rvert$ [cm]	< 20.0	< 20.0	< 20.0	< 20.0

3. Tracking and performance results

In the following plots, a comparison of several distributions and reconstruction efficiencies is shown.

Figure 1 shows a comparison of distributions of the transverse momentum of the reconstructed track $p_{\mathrm{T}}^{\mathrm{reco}}$ for the pp and HI samples. The distributions are normalised to unity. In the HI events, the reconstruction requirements allow for reconstructing a larger number of tracks with $p_{\mathrm{T}}^{\mathrm{reco}} < 1.0$ GeV.

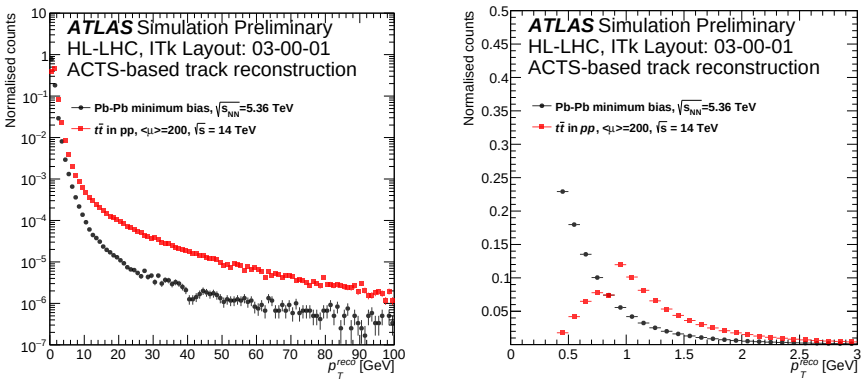

Fig. 1. Transverse momentum, $p_{\mathrm{T}}^{\mathrm{reco}}$, of reconstructed tracks in the HI collisions events (black dots) and $t\bar{t}$ events (red squares) at $\langle\mu\rangle = 200$. A separately normalized and binned version of that histogram in the low-p_{T} region is presented in (b). Distributions are normalised to unity [17].

The impact of different tracking requirements is also visible in figure 2 (a), comparing the pseudorapidity distribution for reconstructed tracks, η^{reco}.

In figure 2 (b), the distributions of track multiplicities are compared. In the pp case, most of the events involve about 2000 tracks and the distribution exhibits a Gaussian shape. For the HI events, the track multiplicity ranges from $O(1)$ to $O(10^4)$. This exhibits how challenging is the track reconstruction of the HI events. About 30% of the HI events contain more than 3000 tracks.

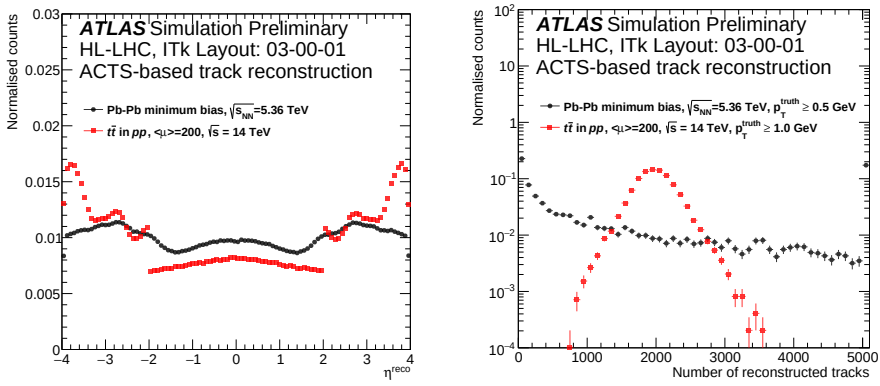

(a) (b)

Fig. 2. (a) The pseudorapidity, η^{reco}, of reconstructed tracks in the HI collision events (black dots) and $t\bar{t}$ events (red squares) at $\langle\mu\rangle = 200$. (b) The multiplicity of reconstructed tracks in the HI collision events (black dots) and $t\bar{t}$ events (red squares) at $\langle\mu\rangle = 200$. For Pb–Pb, the rightmost overflow bin indicates events with a multiplicity higher than 5000 [17]. The distributions are normalised to unity.

In figure 3, the transverse impact parameter resolutions[2] as a function of p_{T} and η are shown. In both pp and HI cases, the higher the track p_{T}, the better the resolution is. Moreover, tracks with low $|\eta|$ have better resolution than the ones with high $|\eta|$. The lower impact parameter resolution obtained in the inclusive HI track sample is driven by the lower-p_{T} cut used in the reconstruction. Optimizations of the HI reconstruction will be pursued over the coming years to improve the efficiency to a similar level as the pp reconstruction. Overall, the resolution values are very good, reaching fractions of millimetres.

[2] For the efficiency and resolution plots, tracks are truth-matched to true particles using a truth-matching probability. This probability is defined as the ratio of the number of hits shared between a track and a particle and the total number of hits on the track. This is the result of material effects; particles with lower momenta tend to be more sensitive to multiple scattering. Pixel hits have a double relative weight with respect to strip measurements [18]. For the $t\bar{t}$ sample, only the tracks from hard scatter events are considered when resolutions and efficiencies are calculated.

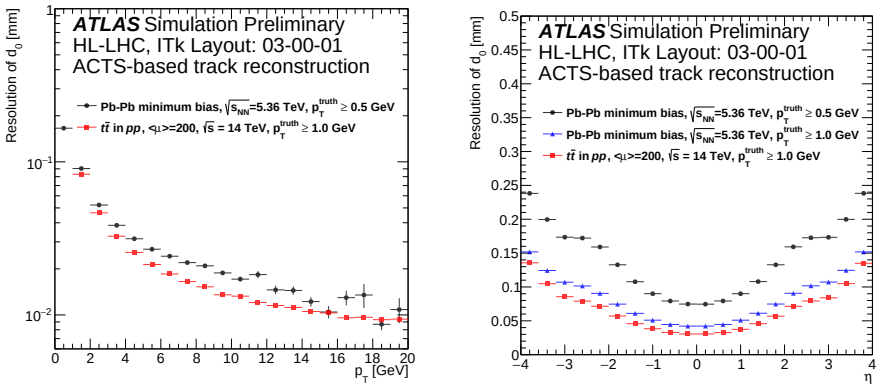

(a) (b)

Fig. 3. The resolution of the transverse impact parameter, d_0, as a function of the truth transverse momentum, p_{T} (a), and truth pseudorapidity, η (b), in the HI collision events (black dots) and $t\bar{t}$ events (red squares) at $\langle\mu\rangle = 200$. Only hard scatter events are considered in the case of $t\bar{t}$ when calculating the resolution. In (b), the resolution achieved specifically for the subset of tracks with $p_{\mathrm{T}}^{\mathrm{truth}} \geq 1.0$ GeV is also displayed [17].

In figure 4, the track reconstruction efficiency is shown as a function of p_{T} and η. The efficiency also depends on track η, reflecting the detector geometry and the tracking requirements.

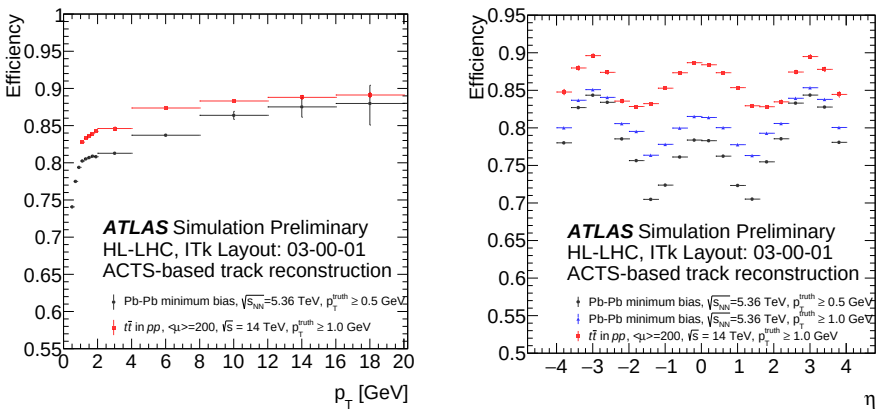

(a) (b)

Fig. 4. Track reconstruction efficiency as a function of the truth transverse momentum, p_{T} (a), and the truth pseudorapidity, η (b), in the HI collision events (black dots) and $t\bar{t}$ events (red squares) at $\langle\mu\rangle = 200$. In (b), the efficiency for the subset of tracks with $p_{\mathrm{T}}^{\mathrm{truth}} \geq 1$ GeV is also displayed [17].

4. Summary

The HL-LHC run will pose new challenges for track reconstruction software. To address this, ATLAS will replace its Inner Detector with a new Inner Tracker which, among other changes, will have higher η coverage. For the track reconstruction software, a cross-experimental toolkit, ACTS is planned to be integrated. It already shows that it is capable of reconstructing both proton–proton and heavy-ion events with reasonable efficiency and resolution, despite vast condition differences of these collisions. The ongoing developments presented in recent years have demonstrated the capabilities of ACTS Toolkit for the ATLAS needs [19]. Further improvements will be done in the next years in preparation of the reconstruction software for Run 4.

This work was supported by the National Science Centre (NCN), Poland under research project UMO-2023/51/B/ST2/00920.

REFERENCES

[1] ATLAS Collaboration, https://cds.cern.ch/record/2922800

[2] O. Aberle *et al.*, https://cds.cern.ch/record/2749422#

[3] ATLAS Collaboration (G. Aad *et al.*), *J. Instrum.* **3**, S08003 (2008).

[4] ATLAS Collaboration, https://cds.cern.ch/record/2285585

[5] A. Xiaocong *et al.*, *Comput. Softw. Big Sci.* **6**, 8 (2022).

[6] ATLAS Collaboration, *Eur. Phys. J. C* **85**, 234 (2025), arXiv:2404.06335 [hep-ex].

[7] S. Frixione, G. Ridolfi, P. Nason, *J. High Energy Phys.* **2007**, 126 (2007), arXiv:0707.3088 [hep-ph].

[8] P. Nason, *J. High Energy Phys.* **2004**, 040 (2004), arXiv:hep-ph/0409146.

[9] S. Frixione, P. Nason, C. Oleari, *J. High Energy Phys.* **2007**, 070 (2007), arXiv:0709.2092 [hep-ph].

[10] S. Alioli, P. Nason, C. Oleari, E. Re, *J. High Energy Phys.* **2010**, 043 (2010), arXiv:1002.2581 [hep-ph].

[11] NNPDF Collaboration (R.D. Ball *et al.*), *J. High Energy Phys.* **2015**, 040 (2015), arXiv:1410.8849 [hep-ph].

[12] X.-N. Wang, M. Gyulassy, *Phys. Rev. D* **44**, 3501 (1991).

[13] ATLAS Collaboration (G. Aad *et al.*), *Eur. Phys. J. C* **70**, 823 (2010), arXiv:1005.4568 [physics.ins-det].

[14] S. Agostinelli *et al.*, *Nucl. Instrum. Methods Phys. Res. A* **506**, 250 (2003).

[15] ATLAS Collaboration (G. Aad *et al.*), *J. Instrum.* **20**, P02018 (2025).

[16] ACTS Common Tracking Software, https://acts.readthedocs.io/en/latest/

[17] ATLAS Collaboration, https://atlas.web.cern.ch/Atlas/GROUPS/PHYSICS/PLOTS/IDTR-2025-01/

[18] ATLAS Collaboration, https://atlas.web.cern.ch/Atlas/GROUPS/PHYSICS/PLOTS/IDTR-2023-04/

[19] ATLAS Collaboration, https://atlas.web.cern.ch/Atlas/GROUPS/PHYSICS/PUBNOTES/ATL-PHYS-PUB-2024-017/